Executive summary

In-flight Lightning Damage Assessment System (ILDAS): Initial in-flight lightning tests and improvement of the numerical methods

Problem area

The results described in this paper form part of the ILDAS-2 project, which Airbus has launched with EADS IW and NLR, as a follow-up to the ILDAS-1 FP6 EU project. The goal of the programme is to develop a system for determining the current waveform and attachment points of lightning striking aircraft in-flight.

Description of work

The ILDAS-2 project focuses on a configuration for measurement during flight tests. For maturation of the ILDAS technology, research

was performed on two parallel paths: in-flight tests were conducted with a simplified system setup on board an Airbus A340 test aircraft flying through lightning, and improvements were made to the numerical methods that perform the required signal processing.

Results and conclusions

The results that have been obtained for both parallel paths are positive, allowing validation to continue with installation of a complete, cabin-only, triggered ILDAS configuration.

This report is based on a presentation held at the International Conference on Lightning and Static Electricity (ICOLSE), Oxford, 6-9 September 2011.

In-flight Lightning Damage Assessment System (ILDAS): Initial in-flight lightning tests and improvement of the numerical methods

Nationaal Lucht- en Ruimtevaartlaboratorium, National Aerospace Laboratory NLR

Anthony Fokkerweg 2, 1059 CM Amsterdam,
P.O. Box 90502, 1006 BM Amsterdam, The Netherlands
Telephone +31 20 511 31 13, Fax +31 20 511 32 10, Web site: www.nlr.nl

NLR-TP-2011-364

In-flight Lightning Damage Assessment System (ILDAS): Initial in-flight lightning tests and improvement of the numerical methods

A.I. de Boer, S.M. Bardet, C. Escure[1], G. Peres[1], V. Srithammavanh[1], K. Abboud[2], T. Abboud[2], J.F. Boissin[3], F. Flourens[3], T. Vorreux[4], L. Riccio[4] and A.P.J. van Deursen[5]
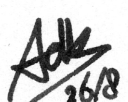
[1] EADS-IW

[2] IMACS

[3] Airbus France

[4] Alten

[5] Technische Universiteit Eindhoven

This report is based on a presentation held at the International Conference on Lightning and Static Electricity (ICOLSE), Oxford, 6-9 September 2011.

Contents

4

In-flight Lightning Damage Assessment System (ILDAS): Initial in-flight lightning tests and improvement of the numerical methods

Alte de Boer, Michiel Bardet
National Aerospace Laboratory NLR, Amsterdam, The Netherlands

Christelle Escure, Gilles Peres, Vassili Srithammavanh
EADS Innovation Works, Toulouse, France

Kamal Abboud, Toufic Abboud
IMACS, Palaiseau, France

Jean-Francois Boissin, Franck Flourens
Airbus France, Toulouse, France

Thibaut Vorreux, Lisa Riccio
Alten SO, Toulouse, France

Alexander van Deursen
Eindhoven University of Technology, Eindhoven, The Netherlands

Abstract

The results described in this paper form part of the ILDAS-2 project, which Airbus has launched with EADS IW and NLR, as a follow-up to the ILDAS-1 FP6 EU project. The goal of the programme is to develop a system for determining the current waveform and attachment points of lightning striking aircraft in-flight. The ILDAS-2 project focuses on a configuration for measurement during flight tests. For maturation of the ILDAS technology, research was performed on two parallel paths: in-flight tests were conducted with a simplified system setup on board an Airbus A340 test aircraft flying through lightning, and improvements were made to the numerical methods that perform the required signal processing. The results that have been obtained for both parallel paths are positive, allowing validation to continue with installation of a complete, cabin-only, triggered ILDAS configuration.

1. Introduction

On average, lightning strikes an individual commercial aircraft about once per year (reference [1]). The desire to know more about the lighting-aircraft interaction resulted in the ILDAS research programme: ILDAS-1 (2006-2009) and ILDAS-2 (2009-2012).

1.1. The ILDAS-1 project

The ILDAS-1 project was an EU-supported FP6 research project to validate the principle of an in-flight lightning strike measurement system. The results were presented during ICOLSE 2007 and 2009 (references [2] and [3]).

In ILDAS-1, a system called ILDAS was defined, developed and successfully verified during both a rig test campaign and a ground test campaign on an A320 aircraft.

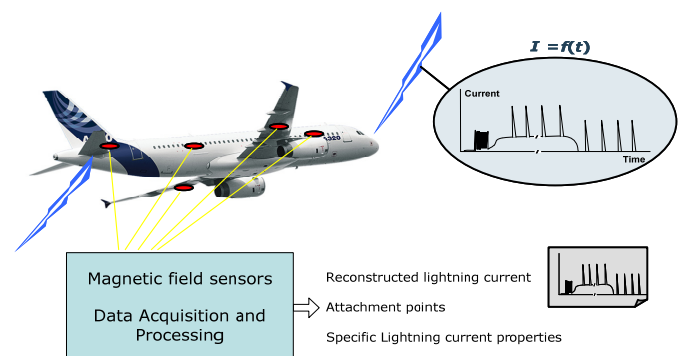**Figure 1 – Reconstruction of the lightning channel current**

The goal of the ILDAS system is to determine the electrical current waveform of the lightning channel and the points of attachment on the aircraft. To do this, synchronous measurements of the magnetic field are performed on various parts of the aircraft (in particular the cabin, the wings and the tailplane) using the specially-developed ILDAS data

acquisition system. The resulting data from multiple sensors is subsequently processed by a numerical toolkit called EM toolkit, which employs an inverse method to determine the (unknown) lightning attachment points and to reconstruct the lightning current waveform.

1.2. The ILDAS-2 project

Airbus decided to continue the ILDAS programme by launching the ILDAS-2 project in 2010 with one primary objective: to use the ILDAS system for the flight test campaign of the all-composite Airbus A350 XWB. The following three benefits are expected:

1. Validation of the ILDAS system's compatibility with an airframe that is mainly composed of composite materials.

2. Improvement of lightning knowledge (medium-term): only a few dozen in-flight measurements of lightning strikes were ever made. ILDAS could measure up to 30 strikes per icing campaign flight, which enables the composition of a comprehensive strike data base. Better knowledge of the phenomenon characteristics will be key to optimize the structural protection of the different zones with respect to the potential impact on airline operations. Beyond pure safety aspects for which current regulation gives satisfaction, this knowledge of the threat statistics would help to define the appropriate protection robustness with respect to airframe maintainability and unscheduled repair.

3. For MROs (long term): a commercial adaptation of the ILDAS system could be installed in airliners and be used as a real-time lightning damage assessment system. It would inform MROs immediately after the strike, thus enabling anticipative maintenance actions. The inspection time can be significantly reduced, as can flight delays and flight cancellations.

To make the ILDAS technology suitable for in-flight measurement of actual strikes to aircraft, it had to be taken from technology readiness level (TRL) 3 ("analytical and experimental critical function and/or characteristic proof-of-concept"), at which the ILDAS-1 project ended, to TRL 6 ("system/sub-system model or prototype demonstration in a relevant environment"). The focus of the project was on delivering an in-flight system with full in-flight measurement functionality (reliable triggering, all sensors installed and data recording without missing strikes), and to post-process and analyse the data on the ground, after the flight.

An ambitious implementation goal was set: make the system cabin-only, meaning a sensor configuration that does not require sensors outside the (pressure and temperature-controlled) cabin, such as on the wings or tail as defined in ILDAS-1. Such a configuration greatly facilitates installation, and relaxes environmental compatibility requirements. Clearly, such a configuration would reduce the amount of information, so it had to be studied how well the waveform reconstruction could be, especially for attachment scenarios involving a wing or parts of the tailplane.

The following significant updates to the ILDAS-1 system were foreseen:

- Performing a trade-off to determine the most suitable strike detection ("trigger") criterion. Options are criteria based on electric field data and/or on magnetic field data from one or more sensors.

- Raising of the stability and reliability of the software (in this case FPGA code) of the controller inside the sensor assembly electronics unit up to a level that is expected from flight test equipment. This code manages all digital functionality, including synchronisation, triggering and acquisition.

- Performing a trade-off to determine the optimal number of sensors and the optimal location of these sensors in the aircraft.

- The determination of the entry and exit points with moving arc (sweeping).

- Improvement of the reconstruction of the lightning current with the inverse method. This reconstruction will have to be done with all lightning current components, and with real and therefore complex lightning current waveforms.

- Ensuring environmental compatibility with the in-flight test environment, in particular electromagnetic compliance, temperature and pressure variations, and mechanical shock and vibration.

1.3. Roadmap of validation test flights

A ground test on an Airbus A320 test aircraft with the concept prototype system with six sensor assemblies was performed in 2009 within the FP6 EU project, as described in reference [3]. In order to incrementally mature the ILDAS system for the flight test campaign of the Airbus A350XWB, a three-step flight test approach was planned:

1. In-flight "engineering testing" with two sensor assemblies, one magnetic-field and one electric-field sensor. The campaign was done to validate the operation of the hardware while in flight and subjected to a true lightning environment. Data from both sensors was continuously recorded for the entire duration of the flight. The campaign was successfully performed on board of an Airbus A340 test aircraft in March 2011, and lead to the capturing of thirty lightning strikes to the aircraft in three flights. The result of this validation step is described in section 2 of this paper.

2. System in-flight validation, using a complete system with a full set of sensor assemblies, and triggered data capture at a high sample frequency. This campaign is foreseen for spring 2012 onboard an Airbus A380 test aircraft. The exact architecture including the trigger criterion and the number of sensor assemblies will be an output of the previous step.

3. Deployment of the validated lightning measurement system on an Airbus A350XWB test aircraft during the icing trials.

With the results of the A350XWB in-flight test campaign, Airbus will then decide to further develop the ILDAS system or not.

2. The first in-flight tests

The first step in the series of planned in-flight tests was an in-flight "engineering test" to validate the system's compatibility with the flight environment, and – more severely – the in-flight lightning environment. In addition, measurement data was produced to allow decisions to be made on various architectural trade-offs. For this initial test a minimum configuration of two sensor assemblies was deployed, one electric-field and one magnetic-field window sensor, both placed in the cabin.

2.1. Detailed characterisation of the magnetic-field window sensor

The novel cabin-window-mounted magnetic-field sensor, which was developed by the Eindhoven University of Technology within the ILDAS EU project (ref. [4], [5], [6]), was further analysed in detail. The measurement principle is that the lightning current generates a magnetic field outside and around the aircraft. A simple but effective sensor to determine that field strength employs the penetration of the field through openings in the fuselage, in particular the cabin windows. A single wire antenna that spans the window at mid-height inside the aircraft senses the magnetic field variation through the window.

Figure 2 – A magnetic-field window sensor installed on one of the windows of an A320 test aircraft during the ILDAS-1 ground test

The antenna calibration depends sensitively on the antenna position and on the shape of the window fixture and flanges. A detailed analysis is given in reference [7]. In the A320 ground tests, the window sensor measurements corresponded to an accuracy of better than 5% with magnetic field due to the injected current in the aircraft.

2.2. Goals of the test

The goals of the in-flight "engineering test" were:

1. Verification of the compatibility with the flight environment, and with the in-flight lightning environment, for the ILDAS hardware (sensors, electronics units and data acquisition computers).

2. In-flight verification of the measurement performance of the electric field window sensor and data acquisition.

3. Generation of data that allows a decision to be made on the optimal lightning strike detection (trigger) algorithm.

2.3. Architecture

The ILDAS system is designed for triggered measurement of lightning-induced fields at an acquisition rate of 100 MS/s for a duration of 1.2 seconds. However, no flight-proven trigger algorithm existed, so the engineering test phase was based on measuring continuously throughout the entire flight, with a reduced amount of data.

Two sensor assemblies, re-used from the ILDAS EU project, were deployed in this test; one for magnetic-field and one for electric-field, see Figure 3.
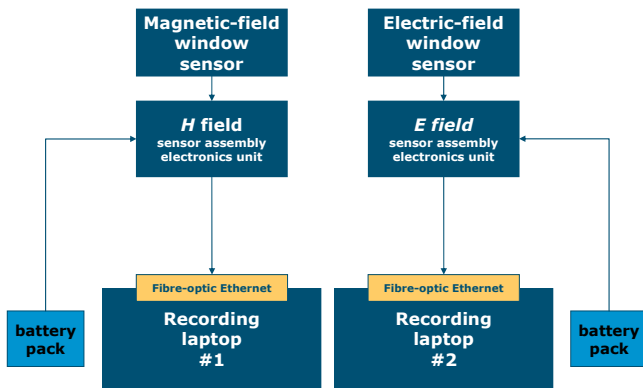

Figure 3 - Architecture for the engineering test phase

Each sensor assembly contains two high-frequency acquisition channels with different gains to reach a wide dynamic range of about 96 dB.

The bandwidth of each sensor channel is:

Magnetic-field sensor: HF1&2   100 Hz – 10 MHz
Electric-field sensor: E1:   100 Hz – 500 kHz
                       E2:   100 kHz – 1 MHz

The sensor assemblies' low-frequency acquisition channel (160 mHz – 100 Hz) was not used.

The field-programmable gate array (FPGA) inside the electronics units down-samples the 10 ns-sampled data to intervals of 2.5 μs. The resulting data was continuously streamed over a 100 Mb/s fibre-optic Ethernet link to a Linux-based data storage computer. For each reporting period of 2.5 μs, the following parameters were recorded:

1. maximum value   (for each HF channel)
2. minimum value   (for each HF channel)
3. average value   (for each HF channel)
4. extreme value (max or min), filtered for spikes, as a backup in case measurements would be disturbed by spurious errors.
5. the results of a candidate trigger algorithm

2.4. Equipment modifications

For the test, the FPGA was reprogrammed to the functionality described above, and for the PCs data recording software was developed that could keep up with the continuous large volume of data.

The system hardware was prepared for installation in the aircraft cabin. This is a relatively benign environment, so environmental adaptation was not a major effort. It consisted of ruggedisation of sensors, sensor assembly electronics, laptops and battery packs, to ensure their correct behaviour when subjected to normal operational shocks and vibrations. To ensure that the equipment does not pose a threat to other aircraft systems, electro-magnetic compatibility measurements were performed on the sensor assembly electronic units and sensors in NLR's EMC facility, in accordance with the procedures described in section 21 of the EUROCAE ED-14F / RTCA DO-160F standard (reference [8]). The equipment passed the test.
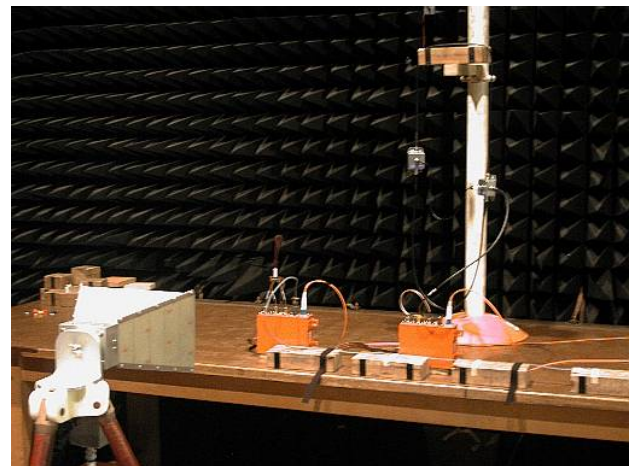

Figure 4 – Two sensor assemblies undergoing emission testing. The electric-field sensor assembly is on the left, the magnetic-field assembly is on the right.

2.5. Installation in the aircraft

Airbus performed the installation of the ILDAS measurement equipment in the Airbus A340 factory test aircraft. The position of the equipment in the aircraft was in the left forward part of the cabin, about half-way between the nose and the leading edge of the wing. In the picture below, the left window contains the magnetic-field window sensor and the middle window the electric-field window sensor. Below the windows is a mounting frame for the two sensor assembly electronic units (orange boxes). Mounted on the cabin floor is a rack with the two data recording computers.
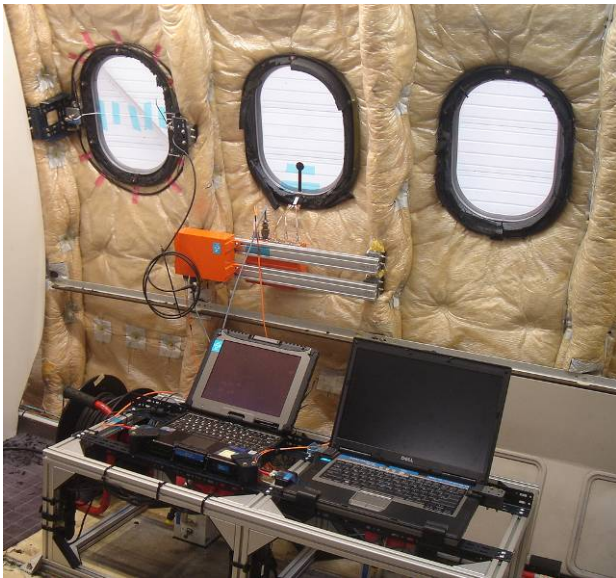

Figure 5 - Installation of the 'engineering test setup' in the Airbus A340 aircraft.

2.6. Flight test results

In March 2011, three lightning flights were performed, lasting between four and six hours, on which ILDAS was on board and active. ILDAS was also enabled on one non-lightning flight, to further characterise background levels. The flight test campaign resulted in 30 lightning strikes to the aircraft, leading to 944 GiB of measurement data. The data was analysed primarily from the perspective of system validation, not from the perspective of research into interaction between lightning and aircraft. This may be done later.

2.6.1. Synchronisation

The measurements of magnetic and electric field were performed independently. The existing ILDAS high-accuracy synchronisation provision could not be used in this engineering setup. Therefore the results were afterwards synchronised by hand, using visual judgement of similarities. It was found that (a) a single correction for a constant frequency difference between the clock oscillators in the electronics, and (b) a constant offset for each flight, resulted in good synchronisation of the results.

2.6.2. Overview of the complete flight

The following figures show an overview of the measured waveforms for the complete flight. For each data point, a line is plotted from the minimum value in that interval to the maximum value. The units on the *x* axis are seconds. The units on the *y* axis are arbitrary units (unscaled output values of the analogue-to-digital converter).

The first flight took place on 15 March 2011 and lasted 4:02 hours, or 14520 seconds. Four strikes were captured, which can be clearly identified from the magnetic-field data plot, but not so easily distinguished from the much more variable data in the electric-field plot.
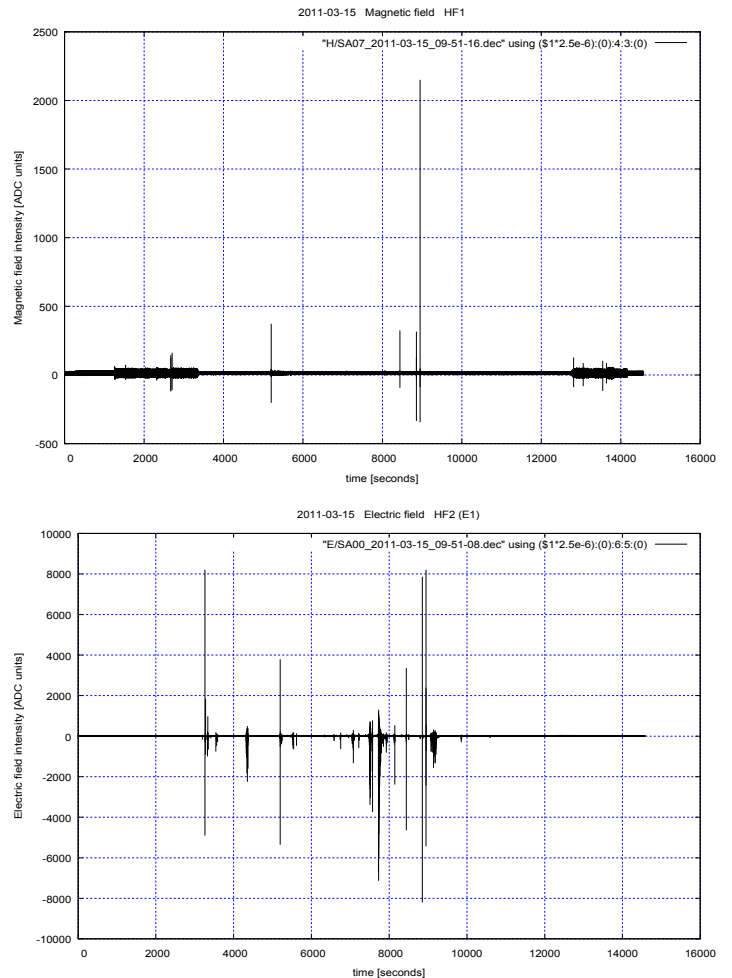

Figure 6 - Overview of the first lightning flight; magnetic field HF1 above, electric field E1 below

The second flight took place on 28 March 2011 and lasted 5:27 hours (19625 seconds). Fourteen strikes were captured.

2011-03-28 Magnetic field HF1
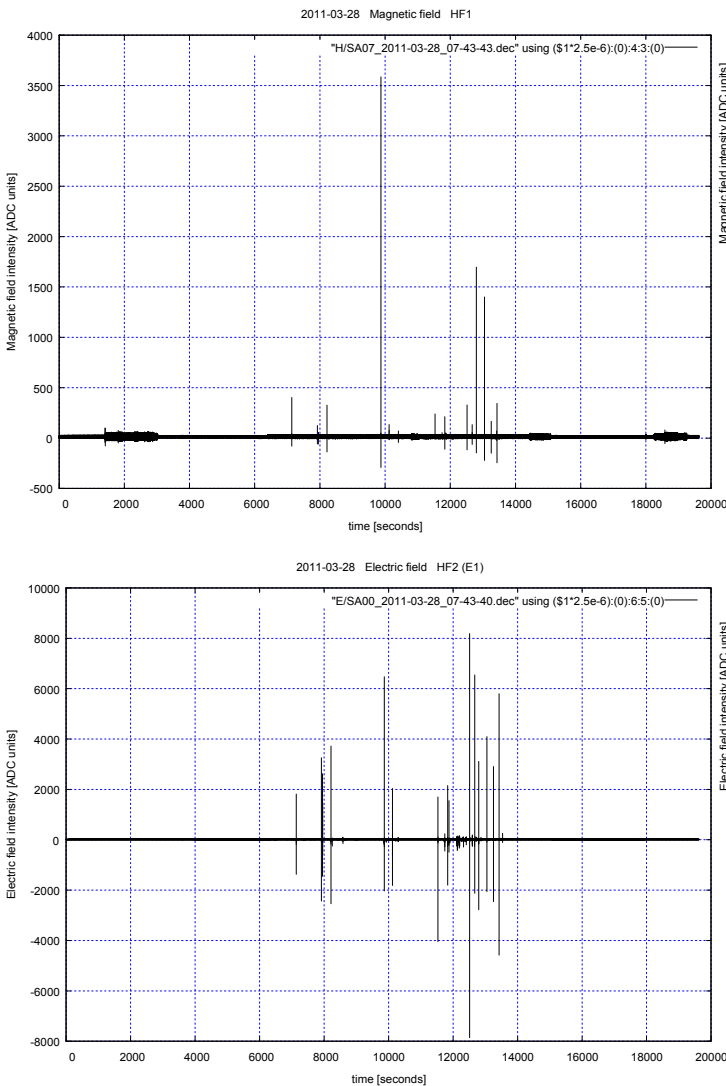

2011-03-28 Electric field HF2 (E1)

Figure 7 - Overview of the second lightning flight; magnetic field HF1 above, electric field E1 below

The third flight took place on 29 March 2011. The sensor assembly batteries could not be recharged before this flight. Consequently, the magnetic-field acquisition stopped after 2:13 hours (7906 s). Acquisition of the electric-field data continued until the end of the flight, for 4:19 hours (15526 s). Twelve strikes were recorded in total, four before the battery depletion and eight after that moment.
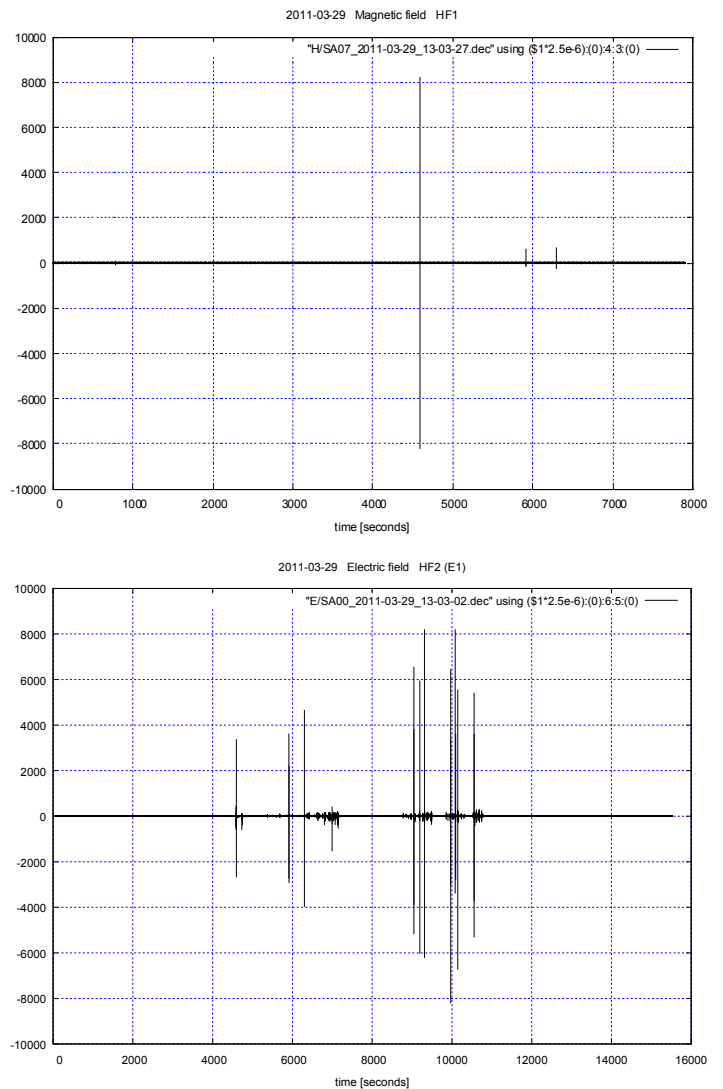

2011-03-29 Magnetic field HF1

2011-03-29 Electric field HF2 (E1)

Figure 8 - Overview of third flight; magnetic field HF1 above, electric field E1 below. Note dissimilar *x* axes.

2.6.3. Strike details, at 200 ms scale

The results are still under detailed analysis. Some early results are shown in the figures below.

The time span (time from left to right in the figure) is 200 ms. The figures consist of magnetic-field data at the top, and electric-field data at the bottom. The magnetic-field data is measured by the HF1 channel (better amplitude resolution, lower dynamic range). For the electric-field data both channels are displayed. The black line is the wideband signal (100 Hz - 500 kHz) with its units on the left axis in black; the red line is the small-band high-frequency signal (100 kHz - 1MHz) with its units on the right axis in red.

The units on the *x* axis are seconds. The units on the *y* axis are arbitrary units (unscaled output values of the analogue-to-digital converter).
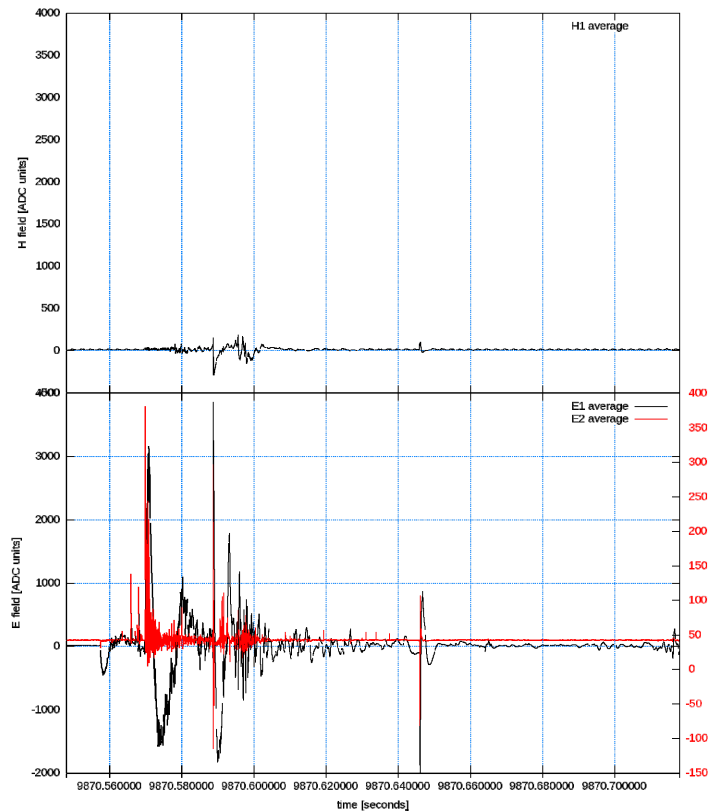

Figure 9 - A lightning strike is preceded by intense electric-field activity (possibly due to a strike at a different location on the aircraft).
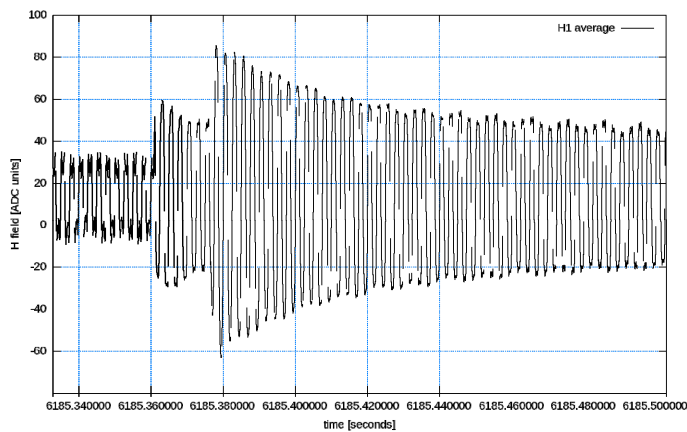

Figure 10 - An example of a non-lightning event. The aircraft fuselage carries return currents from aircraft electrical systems. This current is also measured by the ILDAS magnetic-field sensor and constitutes a background signal. Of course, triggering on these signals must be prevented.
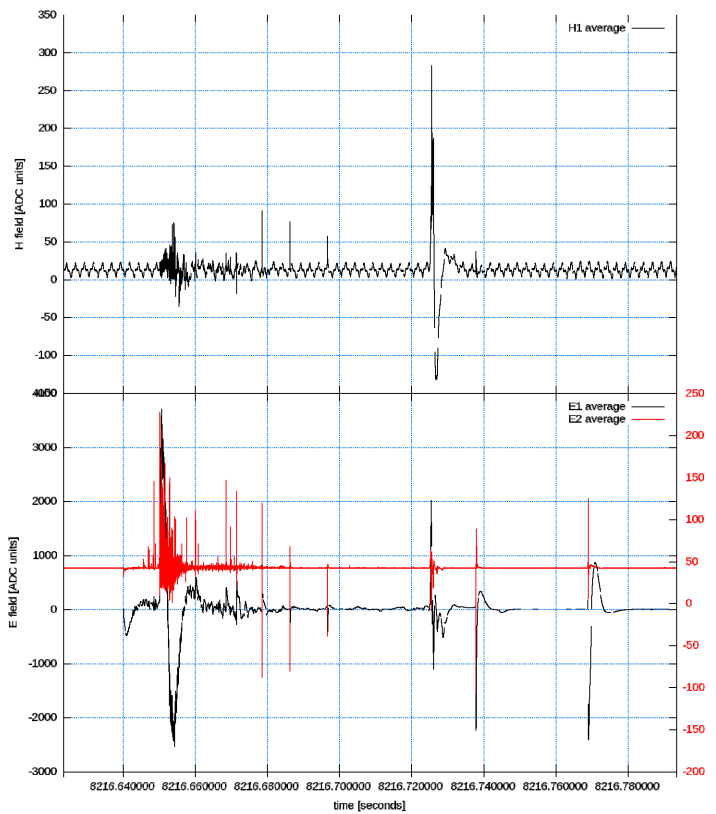

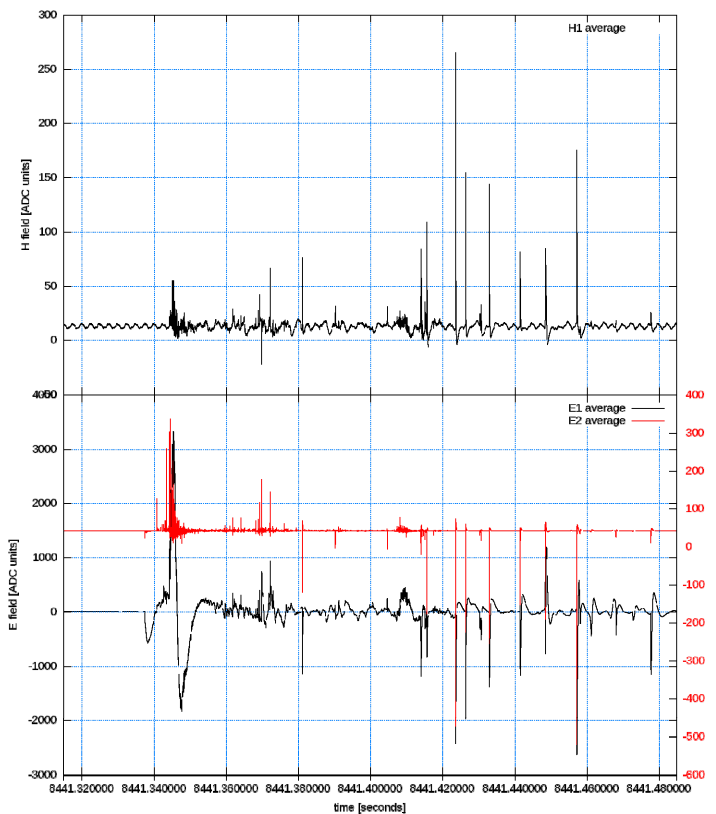**Figure 11 - Here, the main discharge is preceded by lower-level high-frequency magnetic-field activity.**

Figure 12 – A strike consisting of multiple strokes

11

2.6.4. Strike details, at 40 ms scale

The following figures contain waveforms with a time span of 40 ms. The waveforms contain 16 000 samples in that period.
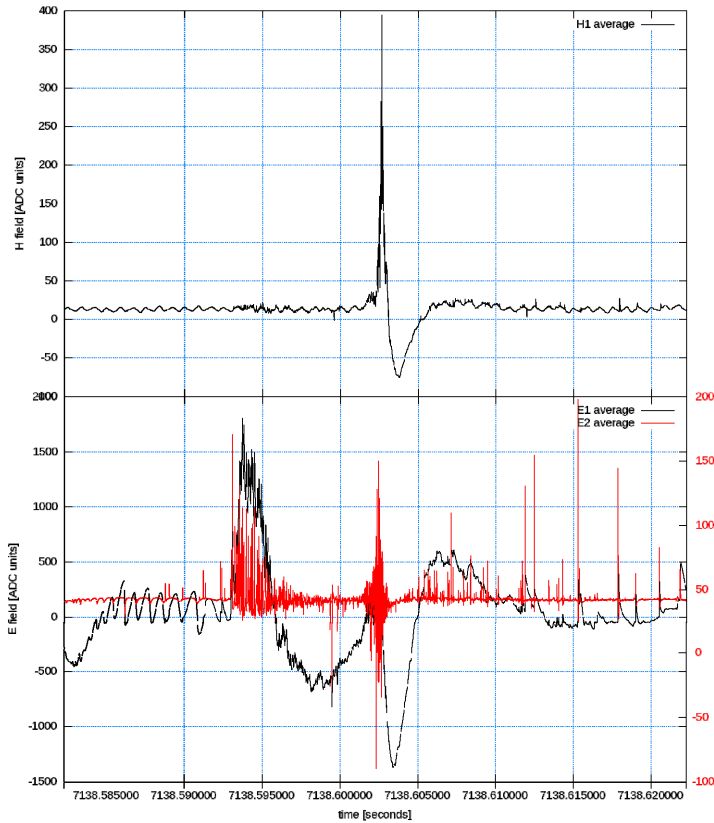

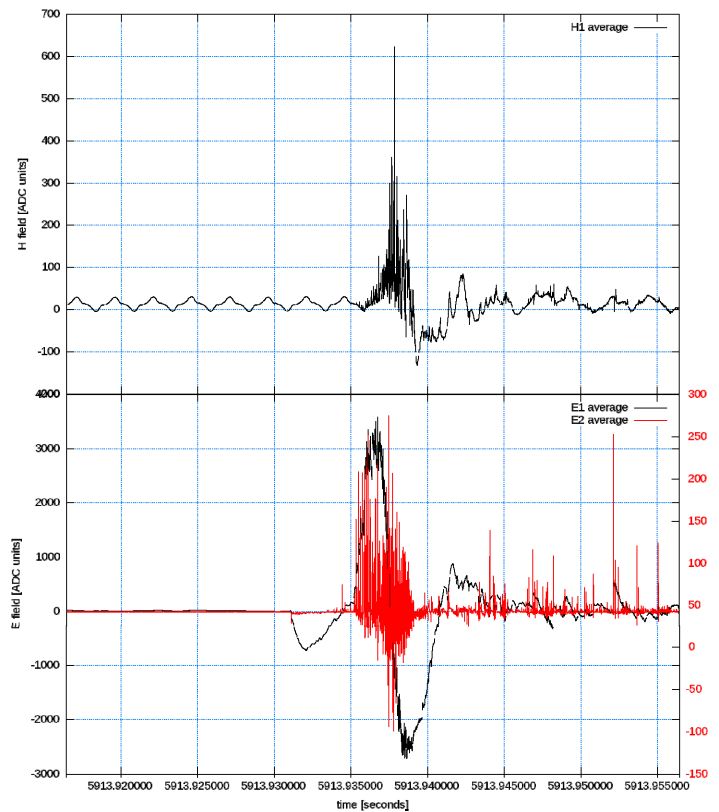**Figure 13 - Intense electric-field activity accompanies a discharge.**

Figure 14 - A strike consisting of many discharge strokes or bursts.

2.6.5. Strike frequency

The continuous recording yields valuable input for the ILDAS system architecture. One unexpected finding was that the frequency at which the strikes to the aircraft occurred was higher than expected. At a certain point in the flight campaign, six strikes were recorded in a period of 1000 seconds, so on average 167 seconds between strikes. This means that a triggered system must be capable of collecting the strike data from all sensors and free the system well within this time period. The ILDAS system architecture was based on a worst-case scenario of two strikes in quick succession, followed by a relatively long time of lightning inactivity, allowing the system ample time to process the captured data. For an application in commercial flights, where pilots try to avoid lighting storms, it may be argued that this is still a valid assumption, but it is now clear that it is not a valid assumption for flight test application. With this finding, the architecture will be adapted to prevent losing data during future campaigns that use triggered acquisition. The adaptation will probably consist of the installation of multiple DADS computers so that data from multiple sensor assemblies can be downloaded in parallel.

2.7. Conclusions on the initial flight tests

The engineering test flight campaign was very successful, with good-quality data recorded for multiple flights, and many lightning strikes experienced. The method to capture statistical parameters over time intervals worked well. The system hardware was successfully validated, with all equipment performing according to expectations, with the possible exception of one battery depletion due to non-fundamental reasons.

The data that was recorded gives valuable input for the ILDAS system architecture, for incorporation in the upcoming A380 flight test configuration, in particular with respect to trigger algorithms. In that test, the system will consist of a full set of sensor assemblies, probably nine, and focus on validation of a triggered system, that is capable of acquiring lightning data at the full sample rate of 80-100 MHz, instead of the reduced rate of 400 kHz, which was the maximum with the continuous data streaming concept employed in the engineering test campaign on the A340.

3. Improvement of the numerical methods

In parallel to the in-flight tests, the post-processing tools were analysed and improved in relation to their status at the end of ILDAS-1.

For the purpose of measured data interpretation and lightning strike reconstruction, a numerical inverse method was developed to retrieve from the measurement of the induced magnetic field on the aircraft skin:

- the initial entry and exit point of the strike

- the amplitude and waveform of the lightning strike current at the attachment point.

One of the first objectives is demonstration of suitability of the system to flight test campaigns and to support the system installation by optimizing the number and position of a set of sensors on the aircraft. Concerning the latter, it has to be noticed that the initial optimum sensor configuration proposed during the ILDAS-1 project has been updated due to the ILDAS-2 project goal to prevent sensors on the wing or tail.

3.1. The Inverse Method

We present in this section the main theoretical principle of the inverse method developed during ILDAS and improved during ILDAS-2. All the results presented in this paper have been obtained with this modified method. The objective of the ILDAS inverse method is to find the most probable lightning scenario, i.e. entry and exit point and the amplitude and waveform, knowing its effect on a given set of E/H field sensors.

3.1.1. Construction of the database : the direct problem

Given an entry point, an exit point and a waveform, the signal measured by the sensors is computed using EADS ASERIS-FD™ software based on a Finite Difference Time Domain (FDTD) solver.

For a given scenario, a couple (entry point, exit point) labeled j, this solver provides an operator

$$f_j : p \mapsto f(p) = \begin{pmatrix} f_{1j}(p) \\ \vdots \\ \vdots \\ f_{Nj}(p) \end{pmatrix}$$

where p is the waveform, a function of time, which is discretized with a given time step δt:
$(p(i\delta t))_{i=1,NT}$

N is the number of sensors, and $f_{ij}(p)$ is the E/H field component computed at the ith sensor, which is also a function of time. The function f computes the so-called *direct problem*. We use this procedure to build a database of synthetic measurements, on a given aircraft model, for a certain number of scenarios, with a given waveform, e.g. a Gaussian pulse.

3.1.2. The inverse problem

Measurements are assumed to be available on N sensors. We note them:

$$m = \begin{pmatrix} m_1 \\ \vdots \\ \vdots \\ m_N \end{pmatrix}$$

m_i is a discretized function of time $(m_i(n\Delta t))_{n=1,Nt}$

The inverse problem has to find for each scenario in the database the best parameter p so that its effect $f(p)$ is as close as possible to the measurements m. For the scenario labelled *j*, we minimize the functional J:

$$J_j(p) = \frac{1}{2}\sum_{i=1}^{N}\left\|f_{ij}(p) - m_i\right\|_{L^2}^2$$

If we denote by p_j^* the solution of this minimization problem, $J_j(p_j^*)$ is the inversion error for this scenario. We use this error as a criterion to choose the most probable scenario : the one that minimizes the inversion error. This problem can be solved directly in the time domain or in the frequency domain by using Parseval's identity.

3.1.3. Limitation of a time-domain resolution

As the problem is linear, we only need to compute the impulse response $h(t)$ with ASERIS-FD™. The E/H fields on the sensors due to any given current source $p(t)$ is given by the convolution product:

$$f(t) = (h * p)(t)$$

For each iteration of the optimization process, this enables to perform simple convolution products instead of direct and computationally costly 3D FDTD calls. This method has been implemented in ILDAS-1 but it turned out that the computational cost of convolution products still remained very high as the number of unknown samples $(p(i\delta t))_{i=1,NT}$ is huge (several millions).

3.1.4. Frequency-domain formulation

Solving the inverse in the frequency domain is much simpler as time convolution becomes a simple product:

$$f(t) = (h * p)(t) \Leftrightarrow F(\omega) = H(\omega) \cdot P(\omega)$$

where $H(\omega)$ is the Fourier transform of the impulse response $h(t)$ and is called the *transfer function*. The problem is decomposed in many simple independent problems, one for each frequency. The solution at a given frequency for a given scenario j has a closed form:

$$p_j^*(\omega) = \frac{H_j(\omega)^* m(\omega)}{H_j(\omega)^* H_j(\omega)} \qquad \textbf{(1)}$$

Finally, applying an inverse Fourier transform gives the time domain signal $(p(n\Delta t))_{n=1,NT}$ of the current source.

3.1.5. Best scenario identification

The inverse method has been improved to be able to determine among a set of given ASERIS- FD scenarios the one that minimizes the error between the provided measurements and the computed data, giving by this way the most likely entry and exit points for the lightning strike.

The error δ_j of the jth ASERIS-FD scenario is defined by:

$$\delta_j = \frac{1}{2\pi}\int_{-\infty}^{+\infty}\Delta_j(\omega)d\omega$$

where

$$\Delta_j(\omega) = \frac{1}{2}\left\|H_j(\omega) \cdot p_j^*(\omega) - m(\omega)\right\|^2$$

is the error between the computed and measured fields at the frequency ω for the jth scenario. Thanks to Parseval's identity,

$$\delta_j = J_j(p_j^*)$$

The index j* of the most likely scenario is obtained by solving the optimization problem hereafter:

$$j^* = \arg\min_j \delta_j$$

3.1.6. Software implementation

The previous theoretical formulation has been implemented numerically. This software works according to the following steps:

1. Creation of the ASERIS FD™ database: for a certain number of scenarios (entry and exit points), a Gaussian or bi-exponential source is used as waveform to generate synthetic measurements at the sensors. The parameters of the source are chosen to satisfy the frequency range of interest.

2. Generation of the transfer matrices: the ASERIS FD™ time-domain numerical measurement are converted into the frequency domain using a Fourier Transform and then normalized by the Fourier Transform of the source. This step provides the transfer matrices $H_j(\omega)$.

3. Processing of measurements: the real measurements (provided by ILDAS sensors) are converted into the frequency domain using a Fourier Transform and in a way to have a frequency sampling similar to the one of the transfer matrices. This step provides the measurements $m(\omega)$.

4. Reconstruction of the optimal source: for each scenario, the optimal source for each frequency is obtained using formula (1). Once done, the optimal current source in the time domain is obtained by inverse Fourier Transform.

5. Optimal solution: comparing inversion errors δ_j, we find the most likely scenario, or scenarios.

3.2. Optimization of the number and position of a set of sensors on the aircraft

The software implementation described above has been applied to provide recommendations on the number of sensors, their type and their location on the aircraft, in order to be able to determine as precisely as possible:

- the initial entry and exit point of lightning

- the amplitude and waveform of the lightning strike at the attachment point.

For this we have to account for several constraints that we can decompose into three different families:

1. One related to the sensor system itself

    - Synchronization of sensors

    - Noise on measurement

    - Sampling of data

2. One related to the lightning strike characteristics

    - Low frequency content, especially the way these characteristics allow to relax some constraints (on the sensors, location, number, …)

    - Impact of sweeping on recording and reconstruction

3. One related to system installation

    - Number and position of sensors : due to many reasons : cost, weight, efficiency, … it is requested to install a minimum number of sensors allowing nevertheless to have a minimum confidence on the scenario prediction and waveform reconstruction

    - The industrial impact of installing sensor assemblies on the wing is so high so that this possibility has been rejected. We have then to adapt the position and number of the sensors on the fuselage and conclude on the capability to predict attachment for example on the engine or the wing tip.

In the following sections we address some of the above constraints.

3.2.1. Impact of desynchronization

POSITION OF THE PROBLEM AND NOTATIONS

The aim of this section is to analyse the impact of desynchronization on the reconstruction of the lightning current. The desynchronisation phenomenon is defined as: any uncertainties in the time relationship between the recordings by individual sensor assemblies. Because accurate synchronisation has been taken into account in the system design from the start, these uncertainties have been kept small. The dominant remaining factor is the variation in time between the reception by the sensor assemblies of the trigger command, and the actual start of recording. This variation exists because the sensor assemblies are independent measurement units that each have

their own clock based on a crystal oscillator. In this way, desynchronisation is limited to about 10 – 20 ns between all sensor assemblies. In this analysis a value of around 20 ns will be used.

The attachment scenario is a nose to right horizontal tailplane; the sensors used are in the figure below:
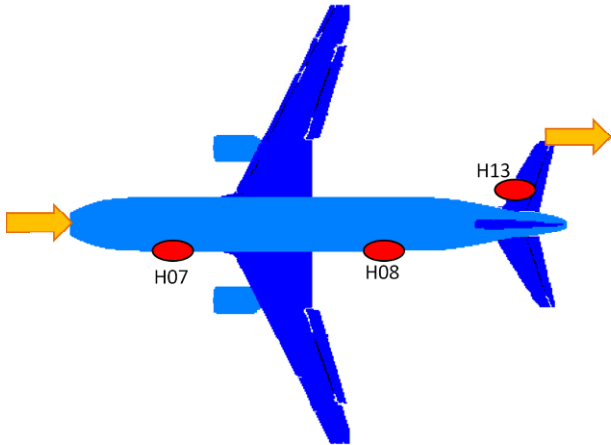

Figure 15

The location of the sensors H07, H08 and H13 came from ILDAS-1 project. The sensor signal data used in this analysis is simulated data, not measured data. The waveforms are type A and H as defined by ED-84, reference [9].

We first make a direct computation and we then introduce desynchronisation on the output signal of one or more sensors to see the capability of the inverse method to reconstruct the input current.

DESYNCHRONIZATION WITH AN A WAVEFORM

This waveform is defined (ref. [9]) by a double-exponential expression:

$$I(t) = I_0 \left(e^{-\alpha t} - e^{-\beta t} \right)$$

Where :
  I_0 = 218 810 A
  α = 11 354 s^{-1}
  β = 647 265 s^{-1}
  t is time (s).
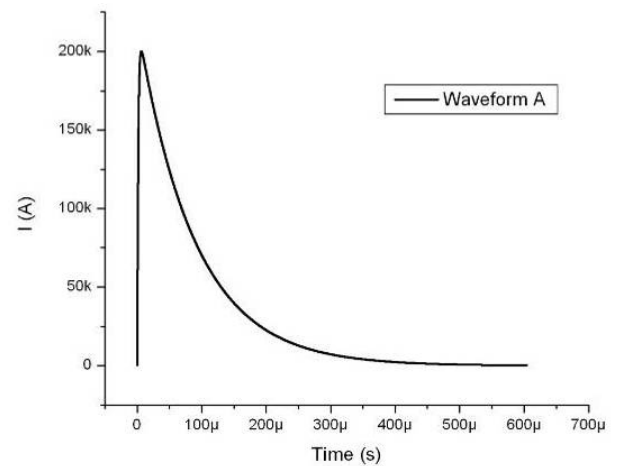
Figure 16

We now desynchronise the signals by delaying the H07 sensor signal by 21.91 ns in relation to the other sensor signals. Then the reconstruction of the current is performed with the EM toolkit. The results are:
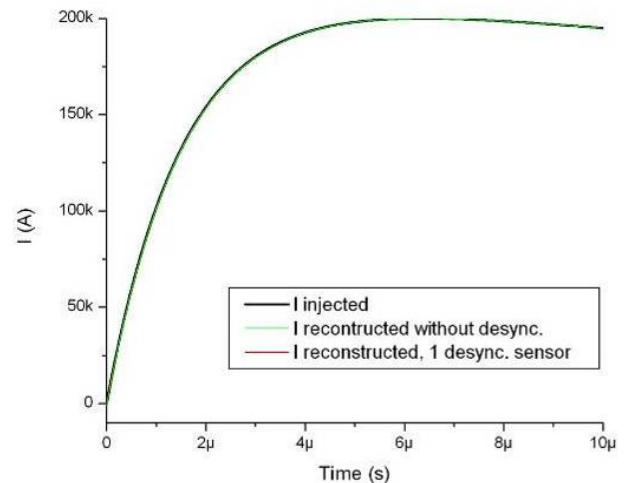
Figure 17

The black curve is the A waveform injected in Aseris-FD, the green one is the reconstructed current by the inverse method when there is no introduced desynchronization. The red curve is the reconstructed current by the inverse method with the H07 sensor desynchronized. As expected because the rise time of this waveform is large compared to the amount of desynchronization, there is no significant impact.

Several other desynchronisation scenarios have been tested and none led to a significant impact.

16

DESYNCHRONIZATION WITH AN H WAVEFORM

This waveform is defined (ref. [9]) mathematically by this double-exponential expression:

$$I(t) = I_0 \, (e^{-\alpha t} - e^{-\beta t})$$

Where :
   I_0 = 10 572 A
   α = 187 191 s^{-1}
   β = 19 105 100 s^{-1}
   t is time (s).

This waveform has a short rise time (100 ns versus 3 µs for the A waveform), which increases the expected impact of desynchronization.
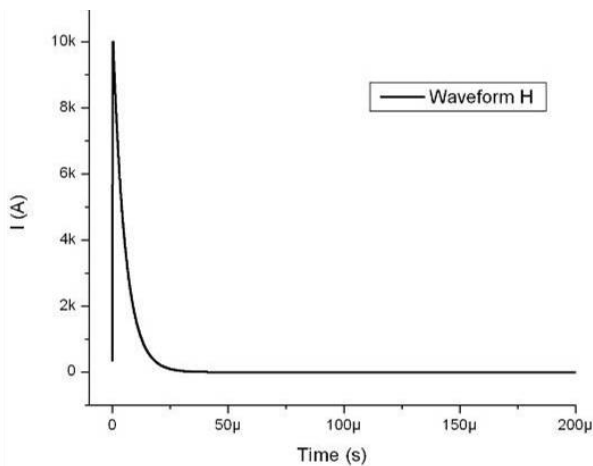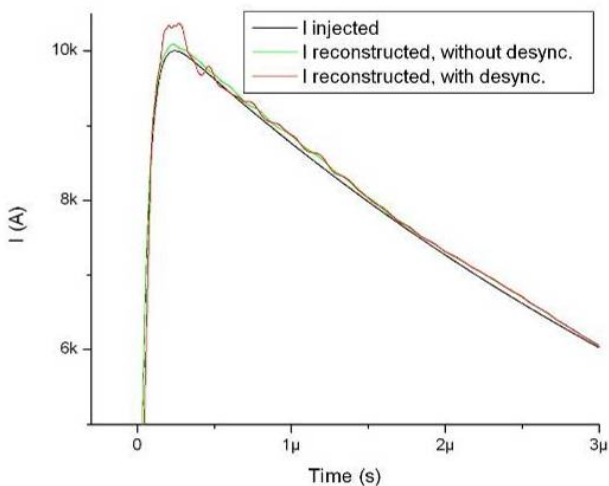

Figure 18

When only the H07 sensor signal is desynchronized by 21.91 ns, the results are:

Figure 19

The black curve is the H waveform injected in Aseris-FD, the green one is the reconstructed current by the inverse method when there is no introduced desynchronization. The red curve is the reconstructed current by the inverse method with the H07 sensor signal desynchronized. As expected

because the rise time of this waveform is 5 times the amount of desynchronization, there is an impact. But this impact is small, localized on the maximum peak of the current, and the reconstruction can be considered as good enough.

When the H07, H13 and H08 sensor signals are all desynchronized by 21.91 ns :
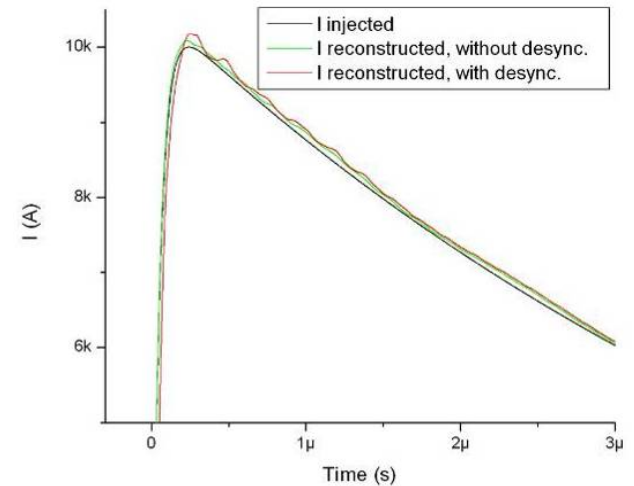
Figure 20

The observations are the same as in the previous case.

To summarise this section, desynchronization has no significant impact if the rise time of the injected current is significantly larger than the amount of the system desynchronization (which is about 20 ns).

3.2.2. Impact of sampling and noise

Like any recording system, the ILDAS sensor system has its own sampling and quantization algorithm and also introduces noise on the recorded signal. The added noise can be considered white (i.e. wide-band) noise with a normal (Gaussian) amplitude distribution. The statistic parameters have been determined from existing measurements, so they includes the effects from the complete measurement chain (sensor, analogue processing, analogue-to-digital-conversion, and digital processing).

As previously with the desynchronisation analysis, we address in this section the possible effect of noise and quantization by adding them to the computed sensor signal and studying the effect on input signal reconstruction by the inverse method.

Since low level input signals suffer more from noise and quantisation then large input signals, several waveform amplitudes will be studied to see if there is a sensitivity threshold.

200 кА

In the figure below, we can see the difference between a pure signal and a noisy + quantized one, for one of the simulated sensor signals (zoomed in on the maximum of its signal).
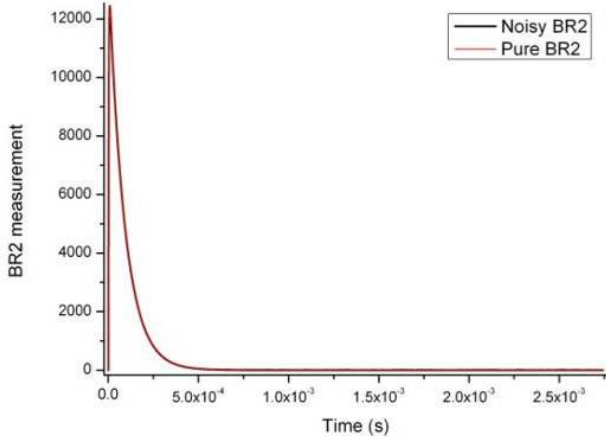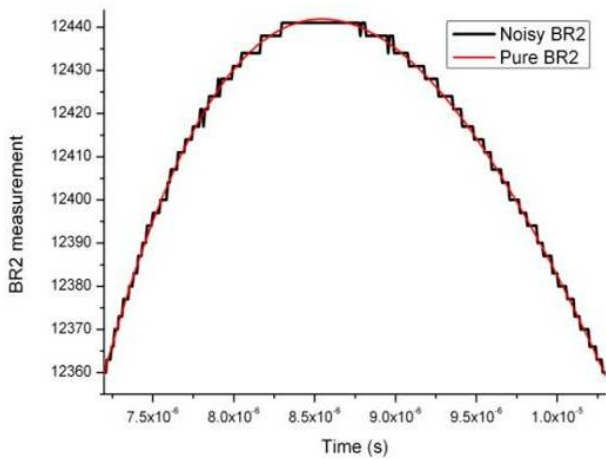

Figure 21

Figure 22

The following figure shows the same difference, in the frequency domain. We can see that noise and quantization have an impact only in high frequencies of signals.
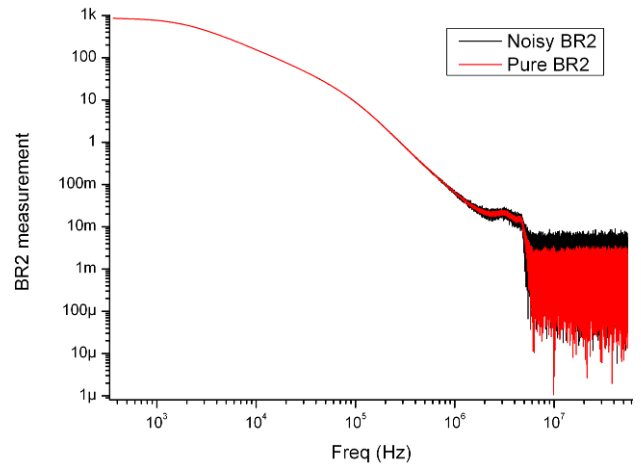

Figure 23

In the figures below, the reconstructed currents from noisy sensor signals (in black), from pure sensor signals (in red) and the pure A waveform are plotted.
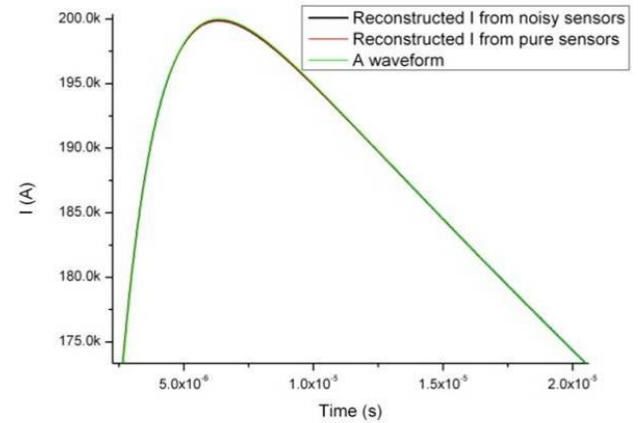
Figure 24

The inverse method reconstruction is really good, we have to zoom in on the peak of the waveform to see the effect of noise:
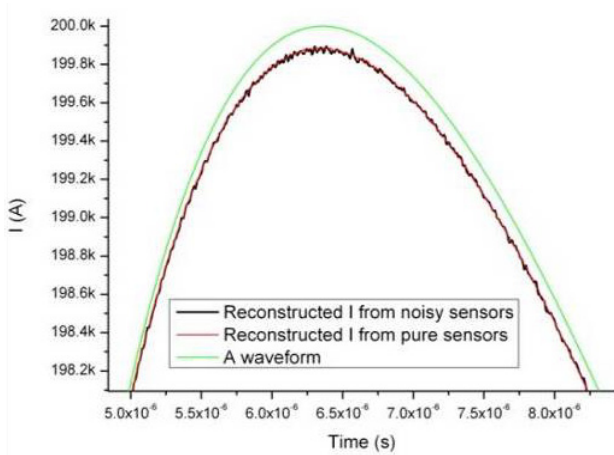
Figure 25

Since a 200 kA amplitude is high in relation to the ILDAS system noise, there is no significant impact on the reconstructed current. A very good reconstruction has also been obtained with the signal as before but with a 20 kA amplitude.

With a 2 kA amplitude signal, the figure below shows the difference for a sensor (located in the right front part of the airplane and labeled FR2 for a right wing tip to left wing tip scenario) without noise and with noise in the temporal domain.
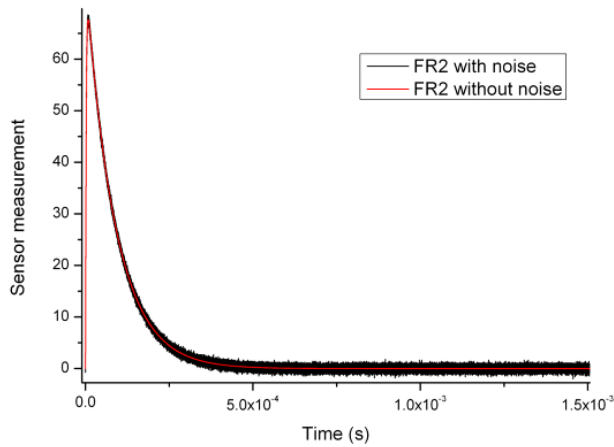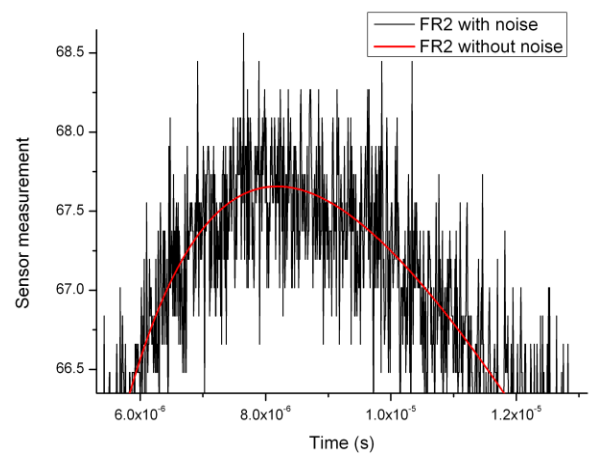

Figure 26

Figure 27

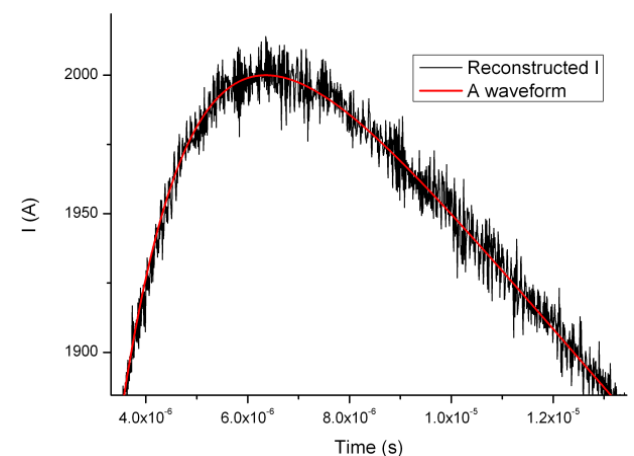The reconstructed signal has then the following shape
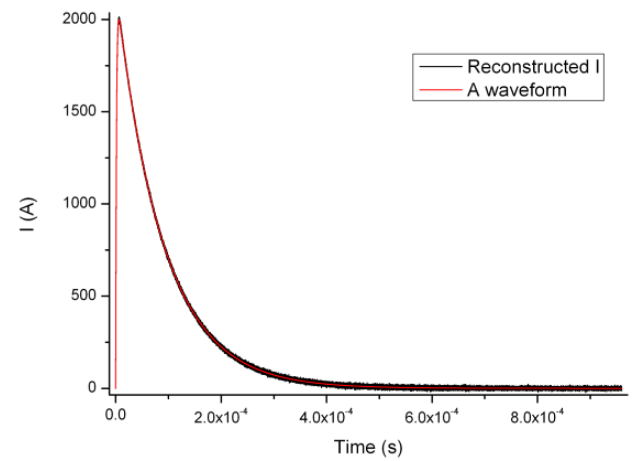
Figure 28

Figure 29

There is an impact of noise, because its amplitude is now non-negligible compared to the 2 kA amplitude A waveform that was injected. Nonetheless, the reconstruction is quite good.

3.2.3. Proposition of a configuration of sensors on the aircraft

The figure below is a diagram of the A320 aircraft on which is shown the location of sensors as specified during the ILDAS-1 project.
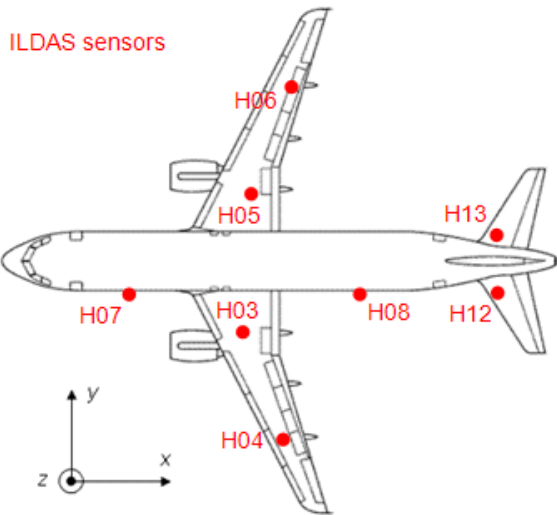

Figure 30

As described earlier, an ambitious goal was set to limit the sensor locations to the pressurised cabin, and therefore to avoid sensors on the wings or in the tail. For the selection of a new set of sensors location, the following three considerations prevailed:

1. Maintain sensors on the front and the back part of the fuselage.

2. Put sensors symmetrically on the right and left part of the fuselage (to have a better indication when the current flows towards or away from the wing),

3. Put sensors at the cross-section of the fuselage and the wings. As for the front/back part sensors, they are placed symmetrically on the right and left part of the airplane. Two of them are dedicated to the measurement of the H field in the x direction, which corresponds to the current flowing along the fuselage. The two others record the H fields along the y axis, which corresponds to the current flowing along the wings. These sensors will be labeled bi-directional sensors.

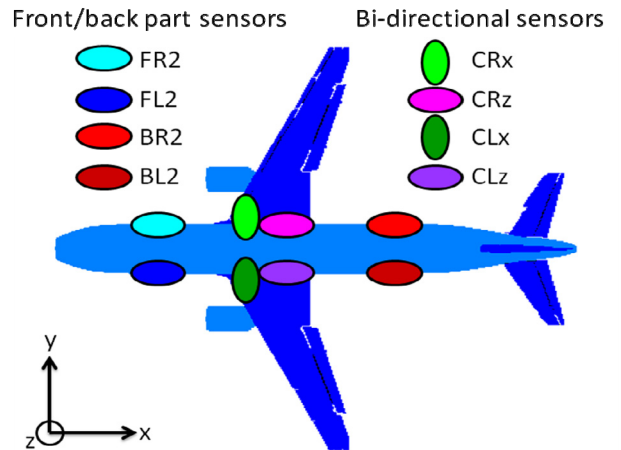This resulted in a configuration with eight sensors. The location of the sensors is shown in the figure below.

Figure 31

NOTATION

The first letter of the sensors name refers to their placement on the airplane :

- F for front part

- C for central part

- B for back part

The second letter indicates the airplane side :

- R for right part

- L for left part

3.3. Lightning entry/exit point scenario and waveform determination

Strictly speaking, each location of the aircraft is a possible attachment point, but the probability is different depending on the area (see ED-91, reference [10]). In the ILDAS-1 project (reference [3]), only the attachment scenarios identified to be of primary importance (19 scenarios) were taken into account. In this study, we took the same scenarios, except those (5) involving the landing gear, as presented in the following table.

20

Table 1

To study the competence of the inverse method to determine the attachment scenario, the lightning waveform and its amplitude, using the proposed set of sensors, we have built a database with those 14 scenarios.

3.3.1. Physical analysis of sensor signals

We considered it important to first perform a physical analysis of the scenario from the sensors signals, to be used as a complementary or alternative analysis to the inverse method results. In what follows, sensors signals will be analysed in the temporal and the frequency domain.

TEMPORAL ANALYSIS OF FRONT/BACK SENSORS

For this study, a 200 kA amplitude A waveform is injected in Aseris. Signals seen by the sensors along the fuselage are plotted in temporal domain, and multiplied by -1 if they are negative, for graph simplicity purpose.
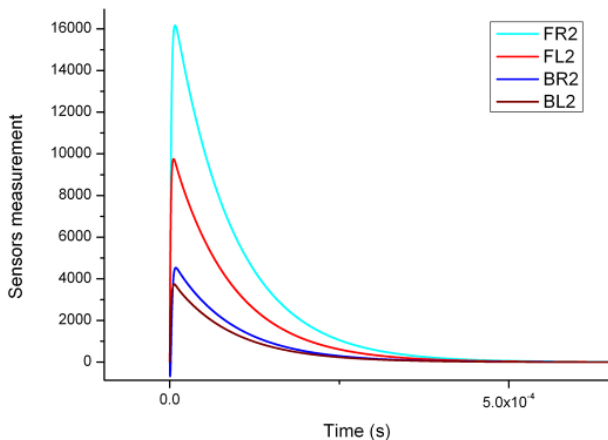

Figure 32 - NOSE TO RIGHT WING TIP

We can see that the front part sensor signals are stronger and asymmetric, indicating an entry point

on the front part of the airplane and a propagation to the right side of the airplane (FR2 stronger than FL2).
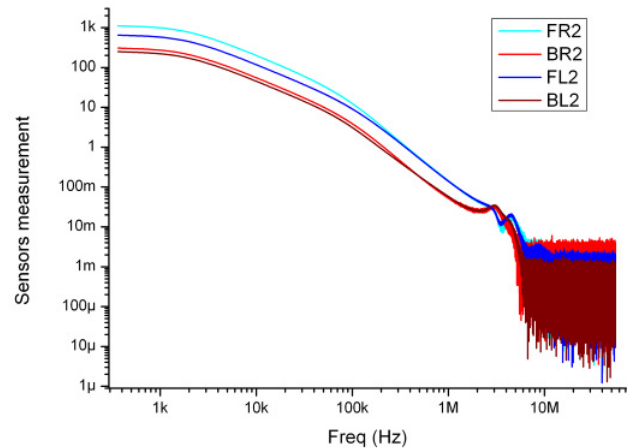
FREQUENCY ANALYSIS OF FRONT/BACK SENSORS

Figure 33 - NOSE TO RIGHT WING TIP

In the frequency domain the previous analysis is still valid : sensor signals on the front part of the airplane are stronger, with a predominance of the right one. We confirmed this with a similar analysis with all other 14 scenarios.

TEMPORAL ANALYSIS OF BI-DIRECTIONAL SENSORS

Now, on bidirectional sensors, we wanted to see if it is possible to perform a physical analysis of the signal, allowing to support the numerical analysis and especially the scenario determination.
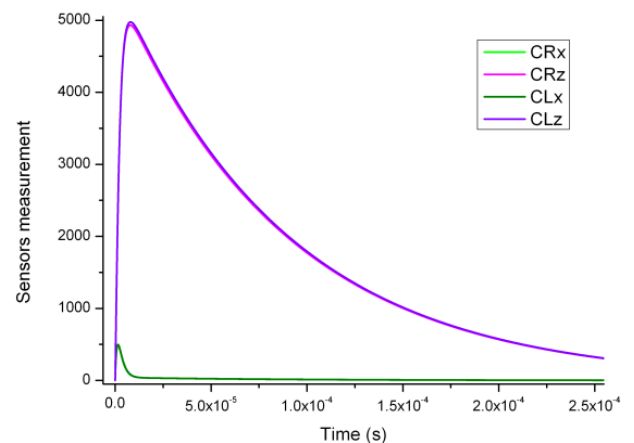

Figure 34 - NOSE TO VERTICAL TAILPLANE

In case of a scenario involving only the fuselage, we can see again two groups of sensors, one for the *x* axis corresponding to the current flowing along the wings (so very weak), and the other for the *z* axis

corresponding to the fuselage. In the first studied scenarios, involving only the fuselage, sensors dedicated to the *z* axis measure the strongest signal.

The sign of sensors signals can also be a help to determine the attachment scenario.

FREQUENCY ANALYSIS OF BI-DIRECTIONAL SENSORS

The observation of the bi-directional sensors in the frequency domain is also helpful to discriminate between different scenarios of attachment. A complete analysis of the 14 scenarios has been done allowing to derive a suitable criterion. One of them is shown hereunder.
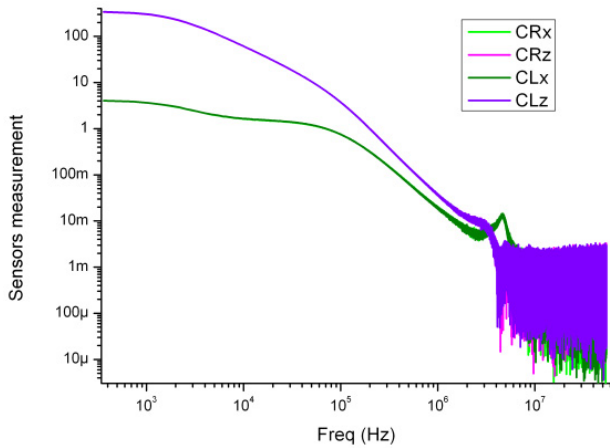

Figure 35 - NOSE TO VERTICAL TAILPLANE

For a nose to vertical tailplane scenario, sensors are grouped by axis. The signals of sensors looking at the *z* axis (along the fuselage) are stronger than the others.

3.3.2. Use of the inverse method to determine scenario and waveform

In this section we are going to present the capability of the inverse method to determine the scenario and to reconstruct waveform and shape of a signal in the two following cases:

- The researched scenario is already stored in the database

- The researched scenario is not in the database

EXISTING SCENARIOS IN THE DATABASE

We will first try to find the good attachment scenario and its reconstructed current from the 8 sensors configuration signals and the database composed of 14 scenarios.

We inject in the inverse method the sensor signals obtained with an injection on the right wing tip and exit on the left wing tip, without noise and quantization. The error criteria found for each scenario are shown in the following table:

Table 2

SCENARIO	ERROR CRITERION
HTPR_VTP	4.664049E-01
HTPR_HTPL	5.214184E-01
REARCONE_HTPR	6.424433E-01
WINGL_ENGINEL	9.962333E-02
WINGR_WINGL	6.968484E-07
WINGL_HTPR	2.037266E-01
WINGR_ENGINEL	2.873522E-02
NOSE_VTP	4.575016E-01
NOSE_HTPR	3.583834E-01
NOSE_REARCONE	4.137114E-01
NOSE_WINGR	2.897257E-01
NOSE_ENGINEL	4.109996E-01
WINGL_HTPL	2.412046E-01
ENGINEL_HTPR	3.951033E-01

HTP = horizontal tailplane, VTP = vertical tailplane

The error criteria pointed out the right attachment scenario, without ambiguity. The figure below shows the reconstructed currents obtained by using the right scenario:
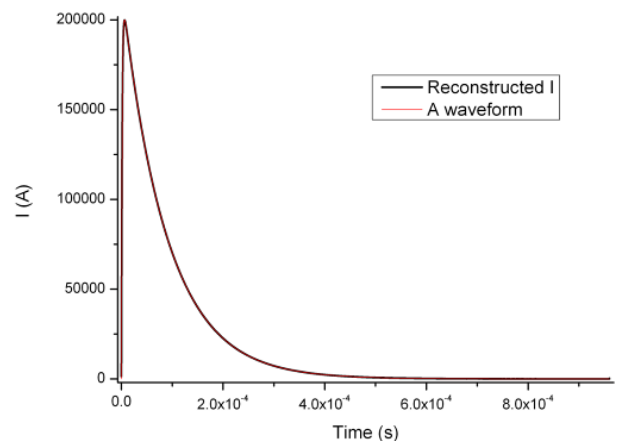

Figure 36

The reconstruction with the right wing tip to left wing tip scenario is excellent. We can see that the inversion error can be a very good criterion to determine the scenario.

MISSING OR "APPROACHING" SCENARIOS

It is also very important to know the inverse method behaviour when the scenario studied is not present in its database.

In the figure below, red squares represent the entry and exit points present in the database. For this test, the rear cone attachment point has been removed from the database. We will feed the inverse method sensor signals obtained with a scenario nose to rear cone. In the figure below, the orange square is the exit point of the studied scenario (which is not stored in the database).
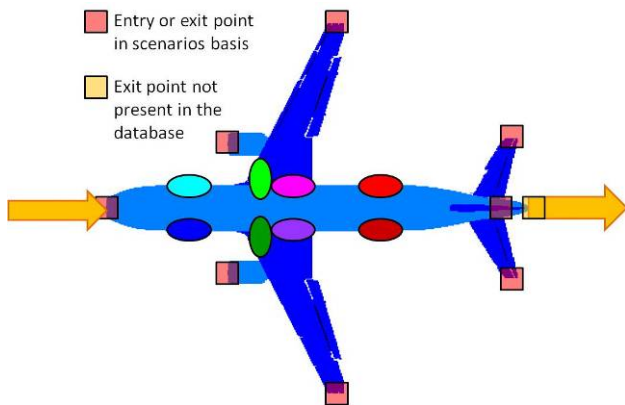

Figure 37

In the next table are reported in the orange lines the lowest error criteria found by the inverse method. The green line is the criteria obtained if we put the right scenario nose to rearcone in the inverse method database.

Table 3

SCENARIO	ERROR CRITERION
NOSE_VTP	1.925701E-05
NOSE_HTPR	1.280380E-04
NOSE_REARCONE	1.213844E-07

It is interesting to plot the reconstructed currents obtained with these approaching scenarios, to have an idea of the spatial precision of the inverse method. In the figure below, reconstructed currents are plotted: the right scenario is the nose to rear cone (in black), and approaching scenarios are nose to vertical tailplane (in blue) and nose to right horizontal tailplane (in green).
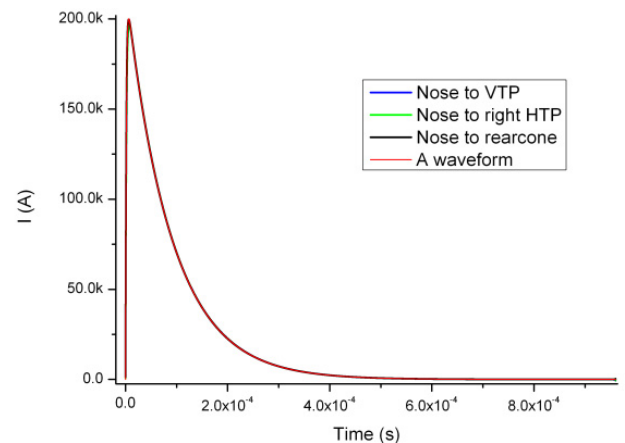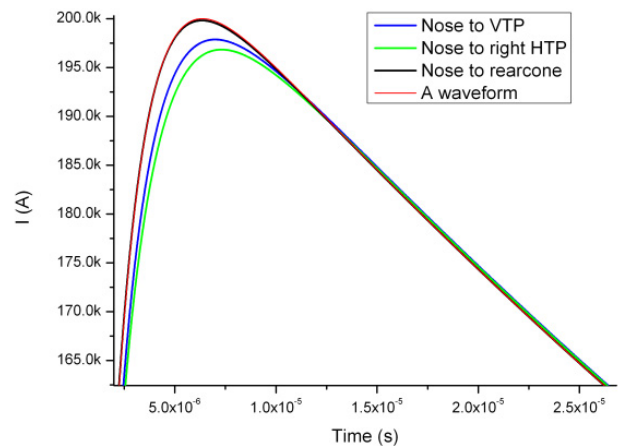

Figure 38

Figure 39

The current reconstruction from these close scenarios is quite good, and give a good idea of the spatial resolution of the inverse method: even if the correct attachment point is not present in the inverse method database, the error criterion pointed out the closest scenario (some meters away from the right location), and the reconstructed current is good.

It is important to note that the spatial resolution of the inverse method does not only depend on the number of sensors, but also on the number and variety of scenarios in its database. So a good way to increase precision on the entry/exit point location determination is not to add additional sensors on the aircraft but to enrich the database with many scenarios.

To confirm this point, we consider a scenario which is not in the database: the entry point is on the nose, and the exit point is between the right engine

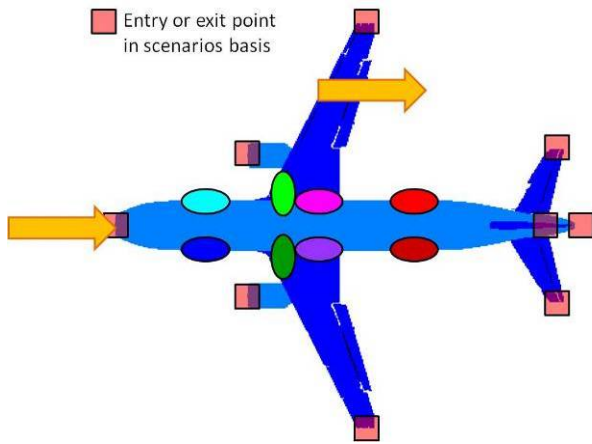and the right wing tip, as shown by orange arrows in the figure below.
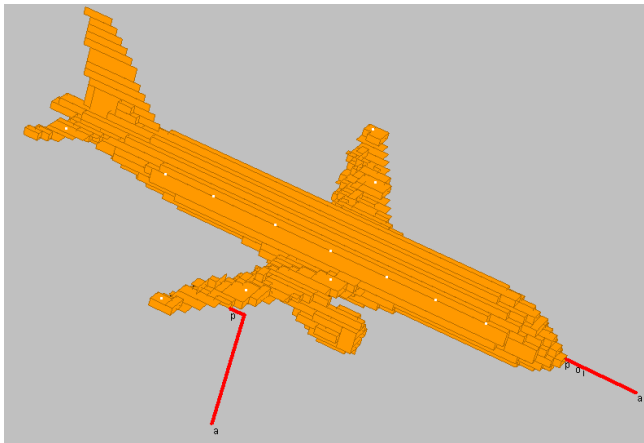

Figure 40

Figure 41

The error criteria given by the inverse method for each scenario are:

Table 4

SCENARIO	ERROR CRITERION
HTPR_VTP	3.644008E+00
HTPR_HTPL	4.353291E+00
REARCONE_HTPR	5.038080E+00
WINGL_ENGINEL	1.886431E+00
WINGR_WINGL	1.817204E+00
WINGL_HTPR	1.715353E+00
WINGR_ENGINEL	2.118652E+00
NOSE_VTP	1.726397E+00
NOSE_HTPR	1.374157E+00
NOSE_REARCONE	1.528339E+00
NOSE_WINGR	6.391790E-02
NOSE_ENGINER	6.631612E-03
NOSE_ENGINEL	9.979938E-01
WINGL_HTPL	2.054136E+00
ENGINEL_HTPR	2.853867E+00

As in the previous case, the two smallest error criteria (nose to right wing tip and nose to right engine, in the orange lines) are close, and there is an ambiguity to determine the correct attachment scenario. We can conclude that the good one is somewhere between these two ones.

The reconstructed current from the nose to right wing tip scenario is plotted in red, from the nose to right engine scenario is in black. The A waveform is in blue.
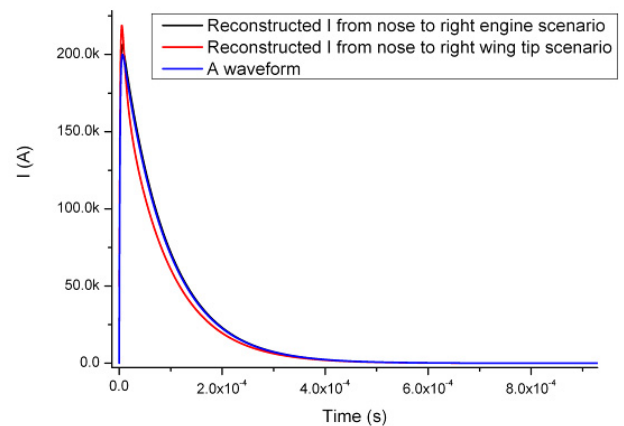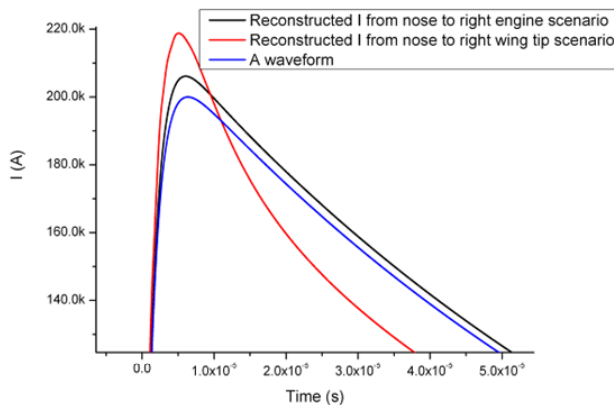

Figure 42

24

Figure 43

This confirms that the spatial resolution of the inverse method does not only depend on the number of sensors, but also on the number and variety of scenarios in its database.

3.4. EM Tool Kit conclusions

During the ILDAS-2 project, major results have been obtained, allowing improving confidence and efficiency of our method to reconstruct lightning strikes. It is worth noting that the conclusions do not depend on the airplane type.

Of course the first crucial step is to have a good representative numerical model of the aircraft, i.e. one that represents well the current distribution for a direct lightning strike.

We have proposed a configuration of eight sensors on the aircraft, accounting for the goal to restrict sensor locations to the cabin. We have shown that the inverse method could function with this constraint and could determine all scenarios including those involving wing or tailplane attachments.

It has been very interesting to quantify the impact of a situation with an entry/exit point that is not stored in the database (what we have called "approaching" scenario, which is probably most representative for real situations). We have seen how the inverse method would return one or more scenarios from the database that are close to the actual scenario.

One of the crucial results that still need to be confirmed with real in-flight data is that increased accuracy can be obtained by enriching the numerical database with more scenarios rather than increasing the number of sensors on the aircraft.

We have also demonstrated the negligible effect of sensor desynchronization and sensor noise on the reconstruction results.

The impact of sweeping could not be evaluated during this period but will be addressed in the near future.

In addition we have also proposed a more physical method to analyze the results directly obtained from the sensors to estimate a possible scenario.

The next phase of the study will address the following points:

- Impact of sweeping

- Analysis with higher frequency signal than waveform A

- Trying to reduce again the number of sensors to check whether we can keep the same conclusions as before while reducing system installation effort, weight and cost.

- Preparation for the next flight test campaign

4. ILDAS-2 conclusions

An important step was made towards the availability of an operational on-board integrated lightning system. The system will be able to record lightning strike events and identify impact locations and strike intensity.

Initial "engineering" in-flight testing with two sensor assemblies, one magnetic-field and one electric-field sensor, was performed. This validated the system's capability to operate in the harsh in-flight lightning environment. About thirty strikes have been recorded at a reduced sampling rate (400 kHz), providing valuable information for the next phases.

Extensive simulations were done with a numerical direct and inverse method, confirming the method's stability and robustness when fed with realistic data aberrations such as noise, quantisation and imperfect synchronisation. An important conclusion is the capability of the inverse method to work with a sensor configuration that consists of cabin-only sensors.

The next step is to validate the system in-flight with a full set of sensor assemblies, which is foreseen for spring 2012 onboard an Airbus A380 test aircraft. The step after that will be target application: the deployment of the validated lightning measurement system on an Airbus A350XWB test aircraft during the icing trials.

4.1. References

[1] M Uman, V Rakov; The interaction of lightning with airborne vehicles. Progr. Aerosp. Sci., vol. 39, p61-81, Oct. 2003.

[2] S Alestra, I Revel, V Srithammavanh, M Bardet, R Zwemmer, D Brown, N Marchand, J Ramos, V Stelmashuk; Developing an in-flight lightning strike damage assessment system. ICOLSE Paris, 2007.

[3] R Zwemmer e.a., "In-flight Lightning Damage Assessment System (ILDAS). Results of the Concept Prototype tests", ICOLSE, 2009.

[4] V Stelmashuk, A P J van Deursen, R Zwemmer; Sensor development for the ILDAS project. EMC Workshop 2007.

[5] V Stelmashuk, A. P. J. van Deursen; Sensors for lightning measurements on aircraft. IEEE Sensors, 2008.

[6] V Stelmashuk, A P J van Deursen; Sensors for in-flight lightning detection on passenger

aircraft. ESA workshop on Aerospace EMC 2009.

[7] A P J van Deursen, "Inductive Sensor for Lightning Current Measurement, Fitted in Aircraft Windows - Part II: Measurements on an A320 Aircraft", IEEE Sensors Journal, Vol. 11, No. 1, January 2011, p.205-209.

[8] EUROCAE, ED-14F, Environmental conditions and test procedures for airborne equipment, March 2008.

[9] EUROCAE, ED-84, Aircraft Lightning Environment and Related Test Waveforms, July 1997 plus amendments of 1999, 2001 and 2006.

[10] EUROCAE, ED-91, Aircraft Lightning Zoning Standard, July 1998 plus amendments of 1999 and 2006.

4.2. Acknowledgements

4.3. Contacts

Alte de Boer — adeboer@nlr.nl
Michiel Bardet — bardet@nlr.nl
Christelle Escure — christelle.escure.external@eads.net
Gilles Peres — gilles.peres@eads.net
Vassili Srithammavanh — vassili.srithammavanh@eads.net
Jean-François Boissin — jean-francois.boissin@airbus.com
Franck Flourens — franck.flourens@airbus.com
Lisa Riccio — lisa.riccio.external@airbus.com